MOLECULAR ONCOLOGY 8 (2014) 401–416

available at www.sciencedirect.com

ScienceDirect

www.elsevier.com/locate/molonc

LIM-homeobox gene 2 promotes tumor growth and metastasis by inducing autocrine and paracrine PDGF-B signaling

Aleksandar Kuzmanov[a,1], *Ulrike Hopfer*[a,b,1], *Patricia Marti*[a,b], *Nathalie Meyer-Schaller*[a], *Mahmut Yilmaz*[a,c], *Gerhard Christofori*[a,*]

[a]*Department of Biomedicine, University of Basel, Mattenstrasse 28, 4058 Basel, Switzerland*
[b]*Novartis, Basel, Switzerland*
[c]*Roche, Basel, Switzerland*

ARTICLE INFO

Article history:
Received 8 November 2013
Received in revised form
11 December 2013
Accepted 16 December 2013
Available online 25 December 2013

Keywords:
Lhx2
PDGF-B
EMT
Tumor progression
Metastasis

ABSTRACT

An epithelial-mesenchymal transition (EMT) is a critical process during embryonic development and the progression of epithelial tumors to metastatic cancers. Gene expression profiling has uncovered the transcription factor LIM homeobox gene 2 (Lhx2) with up-regulated expression during TGFβ-induced EMT in normal and cancerous breast epithelial cells. Loss and gain of function experiments in transgenic mouse models of breast cancer and of insulinoma *in vivo* and in breast cancer cells *in vitro* indicate that Lhx2 plays a critical role in primary tumor growth and metastasis. Notably, the transgenic expression of Lhx2 during breast carcinogenesis promotes vessel maturation, primary tumor growth, tumor cell intravasation and metastasis by directly inducing the expression of platelet-derived growth factor (PDGF)-B in tumor cells and by indirectly increasing the expression of PDGF receptor-β (PDGFRβ) on tumor cells and pericytes. Pharmacological inhibition of PDGF-B/PDGFRβ signaling reduces vessel functionality and tumor growth and Lhx2-induced cell migration and cell invasion. The data indicate a dual role of Lhx2 during EMT and tumor progression: by inducing the expression of PDGF-B, Lhx2 provokes an autocrine PDGF-B/PDGFRβ loop required for cell migration, invasion and metastatic dissemination and paracrine PDGF-B/PDGFRβ signaling to support blood vessel functionality and, thus, primary tumor growth.

1. Introduction

For a cancer to progress and to metastasize it is thought that tumors need to undergo two critical processes: First, to obtain an adequate supply of oxygen and nutrients primary tumors form functional vascular networks for efficient blood delivery through a process known as angiogenesis (Folkman, 1990). Secondly, tumor cells undergo an epithelial-mesenchymal transition (EMT) to gain migratory and invasive capabilities and to disseminate throughout the body and seed distant metastases (Brabletz et al., 2005; Christofori, 2006; Thiery and Sleeman, 2006). Tumor angiogenesis in most cases produces abnormal and leaky vessels, which actually hampers tumor perfusion (Baluk et al., 2003). Vascular maturation is thus an

Abbreviations: EMT, epithelial-mesenchymal transition; Lhx2, LIM homeobox gene 2; PDGF-B, platelet-derived growth factor.

* *Corresponding author*. Tel.: +41 61 267 35 64; fax: +41 61 267 35 66.
E-mail address: gerhard.christofori@unibas.ch (G. Christofori).

[1] Equally contributing authors.

1574-7891/$ – see front matter © 2013 Federation of European Biochemical Societies. Published by Elsevier B.V. All rights reserved.
http://dx.doi.org/10.1016/j.molonc.2013.12.009

important process to ensure optimal tumor perfusion, usually manifested by the recruitment of pericytes to newly formed vessels (Mazzone et al., 2009). Several signaling pathways have been implicated in pericyte recruitment to the tumor vessel wall, including angiopoietin/Tie2 and PDGF/PDGFR signaling (Hawighorst et al., 2002; Abramsson et al., 2003; Furuhashi et al., 2004; di Tomaso et al., 2009; Nasarre et al., 2009; Fagiani et al., 2011). On the other hand, an EMT usually occurs at the invasive front of solid tumors promoting cancer cell dissociation from primary tumors and metastatic dissemination. A plethora of transcription factors have been identified as critical for an EMT and metastasis formation, including Snai1 (Snail), Snai2 (Slug), Zeb1 (δEF1), Zeb2 (Sip1), E47, Twist, goosecoid, FoxC2, Dlx2, RBPjκ, Yap/Taz, Sox4 and 9, NFkB, and Klf4 (Polyak and Weinberg, 2009; Thiery et al., 2009; Yilmaz et al., 2011; Tiwari et al., 2013a,b).

We here report the increased expression of the transcription factor LIM homeobox gene 2 (Lhx2) during EMT of normal mammary gland and breast cancer cells and its functional role during breast carcinogenesis, notably during tumor angiogenesis and tumor invasion and metastasis. Lhx2 is a member of the LIM homeobox gene family consisting of two zinc-finger domains (Dawid et al., 1995). It has been originally identified in pre-B cell lines and in the central nervous system, for example by promoting pituitary-specific expression of the glycoprotein hormone α-subunit gene (Xu et al., 1993; Roberson et al., 1994). Lhx2 plays a critical role in embryogenesis, as Lhx2-deficient mouse embryos develop liver fibrosis and die at embryonic day E15-17 (Wandzioch et al., 2004). Lhx2 is also essential for the development of the eye, forebrain and erythrocytes (Porter et al., 1997). Lhx2 binds to the homeodomain site of the M71 odorant receptor gene promoter (M71) and is thus required for the development of olfactory sensory neurons (Hirota and Mombaerts, 2004). By regulating the expression of the axon guidance receptors Robo1 and 2, Lhx2 modulates the establishment of specific connections of thalamic neurons (Marcos-Mondejar et al., 2012). Furthermore, Lhx2 is critical for cortical progenitor differentiation forebrain and neocortex development (Chou and O'Leary, 2013; Roy et al., 2013). Lhx2 is also a positive regulator of hair formation (Rhee et al., 2006; Tornqvist et al., 2010). It directly regulates the expression of the *Sox9*, *Tcf7* and *Lgr5* genes in hair follicle stem cells and facilitates epidermal regeneration after injury (Mardaryev et al., 2011). Loss-of-function experiments have revealed an essential role of Lhx2 in the regulation of posterior pituitary development (Zhao et al., 2010). Besides its roles in physiological conditions, Lhx2 is highly expressed in a variety of human cancer types, including cancers of the stomach, germ cell, kidney, skin, soft tissue/muscle tissue, pancreas and in glioma (Breast Cancer Database, http://www.itb.cnr.it/breastcancer/php/geneReport.php?id=9355; Gorantla et al., 2011). However, the functional contribution of Lhx2 to carcinogenesis has remained elusive.

To investigate the role of Lhx2 in EMT and tumor progression, we have performed loss and gain-of-function experiments in transgenic mouse models of cancer *in vivo* and during TGFβ-induced EMT of cultured cells *in vitro*. We here report that Lhx2 supports mammary tumor growth by inducing tumor blood vessel maturation and functionality. Furthermore, Lhx2 promotes tumor cell migration, invasion and metastasis formation. Lhx2 directly induces the expression of the gene encoding for platelet-derived growth factor B (PDGF-B) and thus promotes PDGF-B/PDGFRβ signaling. Our data demonstrate that Lhx2-induced PDGF-B/PGFRβ signaling enhances vessel maturation and tumor growth via a paracrine mechanism and, in an autocrine manner, it promotes tumor cell migration, invasion and metastasis formation.

2. Materials and methods

2.1. *Microarray gene expression profiling*

Microarray gene expression profiling was performed as previously described (Waldmeier et al., 2012).

2.2. *Chromatin immunoprecipitation (ChIP)*

ChIP experiments were performed as previously described (Weber et al., 2007; Tiwari et al., 2013a,b). In brief, crosslinked chromatin was sonicated to achieve an average fragment size of 500 bp. Starting with 100 μg of chromatin and 5 μg of anti-Lhx2 (sc-19344, Santa Cruz), 1 μl of ChIP material and 1 μl of input material were used for quantitative real-time PCR using specific primers covering the promoter of target genes. ChIP with unrelated IgG or primers covering an intergenic region were used as a control. The efficiencies of PCR amplification were normalized to the PCR product of the intergenic region. Primer sequences are presented in Suppl. Experimental Procedures.

2.3. *Kaplan–Meier survival analysis*

Kaplan–Meier survival analyses were performed on 198 lymph-node negative breast cancer patients from the TRANSBIG Multicenter Independent Validation Series (GSE7390) (Desmedt et al., 2007) and 82 advanced breast cancer patients from MSKCC published by Minn et al. (GSE2603) (Minn et al., 2005). Tumors were separated into a high Lhx2 and low Lhx2 expressing group based on the median expression of Lhx2 (Minn database) or kmeans-clustering of Lhx2 expression (TRANSBIG database), and the overall survival or metastasis free survival was compared between these two patient groups. Tumors from the Minn database were further stratified into ER-negative (36 tumors) and ER-positive (46 tumors) tumors based on the available ER status information. Kaplan-Meier survival analysis and Cox proportional hazards regression modeling was performed with the survival package 2.37-2 of R version 2.15.1 (www.r-project.org). Survival differences were considered statistically significant at a p-value from the likelihood-ratio test of less than 0.05.

2.4. *Animal experimentation*

All studies involving mice have been approved by the Swiss Federal Veterinary Office (SFVO) and the regulations of the Cantonal Veterinary Office of Basel Stadt (licences 1878, 1907, 1908).

2.5. Statistical analysis

Statistical analysis was performed using statistical software GraphPad Prism 5 (GraphPad Software Inc, San Diego, CA). Statistical significance was evaluated by Student's *t*-test or Mann–Whitney test depending on the distribution of the data. A p-value <0.05 was considered statistically significant.

3. Results

3.1. *Lhx2 expression is induced during EMT and carcinogenesis*

To identify critical regulators of EMT, normal murine mammary gland (NMuMG) cells (Miettinen et al., 1994; Lehembre et al., 2008) were treated with TGFβ for 10 days and changes in gene expression were assessed. Among a large number of genes, Lhx2 mRNA levels were significantly increased after four days of TGFβ treatment (Figure 1A). Lhx2 expression is also induced during TGFβ-induced EMT in Py2T, a murine breast cancer cell line derived from a tumor of an MMTV-PyMT transgenic mouse (Waldmeier et al., 2012) and in MT cells that have been established from a mammary tumor of an MMTV-Neu transgenic mouse carrying conditional (floxed) alleles of the E-cadherin gene. These cells undergo EMT upon Cre-mediated genetic ablation of the E-cadherin gene (MTΔE-Cad) (Lehembre et al., 2008) (Figure 1A). Lhx2 mRNA levels were not significantly increased after TGFβ treatment of NMuMG cells transiently silenced for Smad4 expression (siSmad4-NMuMG) (Figure 1B), indicating that *Lhx2* gene expression is regulated by canonical TGFβ signaling. Finally, Lhx2 expression is induced during mammary tumor development in MMTV-PyMT and MMTV-Neutransgenic mice and during pancreatic β-cell carcinogenesis in Rip1Tag2 transgenic mice (Figure 1C and D).

Since Lhx2 is found expressed in variety of human cancers, we assessed whether increased expression of Lhx2 correlated with breast cancer progression and metastasis in patients. Analysis of the TRANSBIG and Minn databases of breast cancer (Minn et al., 2005; Desmedt et al., 2007) revealed that high Lhx2 levels correlated with low overall survival and distant metastasis-free survival (Figure 1E and F). Furthermore, in breast cancers expressing estrogen receptor (ER+), high Lhx2 levels correlated with low bone marrow and lung metastasis-free survival (Figure 1G and H).

3.2. *Lhx2 promotes tumor growth and metastasis*

The high expression of Lhx2 during EMT and in a variety of human and mouse cancers motivated us to investigate the functional role of Lhx2 during breast cancer progression in MMTV-PyMT and MMTV-Neu mice. To assess whether Lhx2 is able to promote tumor growth and malignant progression, we generated transgenic mice expressing Lhx2 and luciferase in the mammary gland (MMTV-Lhx2-IRES-luciferase; MLhx2) (Suppl. Figure S1A). These mice did not develop tumors and did not show any apparent abnormalities. MLhx2 mice were crossed with MMTV-PyMT (MPY) or MMTV-Neu (MN) transgenic mice to generate double-transgenic MPY;MLhx2 and MN;MLhx2 mice expressing Lhx2 specifically in breast tumor cells (Suppl. Figure S1B).The transgenic expression of Lhx2 led to the formation of significantly more and larger tumors in both MPY;MLhx2 and MN;MLhx2 double-transgenic mice as compared to MPY and MN single-transgenic control mice (Figure 2A and B). Quantitative RT-PCR analysis confirmed abundant Lhx2 mRNA levels in the Lhx2-overexpressing tumors (Figure 2C). Phospho-Histone 3 (pH3) staining of tumor sections revealed a clear increase in the numbers of proliferating cells in MPY; MLhx2 tumors, while tumor cell apoptosis was not affected by Lhx2 overexpression (Figure 2D and E).

Since MN mice did not develop distant metastasis with high incidence, metastasis formation was studied in MPY mice only. The numbers of microscopic lung metastasis per primary tumor weight (metastatic index) were significantly increased in MPY;MLhx2 mice as compared to MPY mice (Figure 3A). In addition, the numbers of cytokeratin 8/18-positive circulating tumor cells were significantly higher in the peripheral blood of MPY;MLhx2 mice as compared to MPY littermate controls (Figure 3B). Grading of malignant tumor progression according to (Lin et al., 2003) (Figure 3C) revealed an increase in invasive carcinomas in MPY;MLhx2 double-transgenic mice (28.9 ± 3) as compared to MPY single-transgenic mice (13.5 ± 1), while the incidence of adenomas was reduced in MPY;MLhx2 mice (132.6 ± 20) as compared to MPY mice (253 ± 30) (Figure 3D). No difference in the incidence of hyperplasia was detected. Immunofluorescence staining of tumor sections showed mesenchymal N-cadherin expression almost exclusively in the tumor stroma in both MPY;MLhx2 and MPY tumors (Figure 3E). Epithelial E-cadherin expression was detected with high intensities in adenomas and with lower intensities in carcinomas of both MPY;Lhx2 and MPY mice. Notably, a significant overall reduction of E-cadherin-positive staining was observed in tumors of MPY;MLhx2 mice as compared to MPY littermate controls (Figure 3E), consistent with the accelerated tumor progression and increased metastatic index observed in MPY;MLhx2 tumors.

To study the role of Lhx2 suppression on tumor growth, we generated mice lacking Lhx2 specifically in breast tumor cells by crossing MPY mice with MMTV-Cre (MCre) mice and with mice carrying conditional alleles of Lhx2 (MPY;MCre;$Lhx2^{fl/fl}$) (Mangale et al., 2008) (Suppl. Figure S1C). We also generated mice lacking Lhx2 expression specifically in pancreatic β-tumor cells by crossing Rip1Tag2 (RT2) mice with RipCre (RCre) mice and mice carrying conditional alleles of Lhx2 (RT2;RCre;$Lhx2^{fl/fl}$) (Suppl. Figure S1C). Lhx2 depletion in both MPY;MCre;$Lhx2^{fl/fl}$ and RT2;RCre;$Lhx2^{fl/fl}$ mice did neither affect tumor weight nor tumor incidence, although Lhx2 expression was profoundly reduced in Lhx2-deficient breast and β-cell tumors (Suppl. Figure S2A–C). Lhx2-deficient tumors of MPY;MCre;$Lhx2^{fl/fl}$ and RT2;RCre;$Lhx2^{fl/fl}$ mice also did not show significant changes in tumor cell proliferation and apoptosis (Suppl. Figure S2D–G). Even though the numbers of cytokeratin 8/18-positive circulating tumor cells were significantly reduced in the blood of MPY;MCre;$Lhx2^{fl/fl}$ mice as compared to MPY littermate controls, the metastatic index was not

significantly affected (Suppl. Figure S3A,B). In addition, grading of tumor stages revealed no differences in malignant tumor progression and N-cadherin/E-cadherin expression (Suppl. Figure S3C,D) between tumors of MPY;MCre;Lhx2$^{fl/fl}$ and MPY mice. The lack of Lhx2 expression in RT2;RCre;Lhx2$^{fl/fl}$ mice also did not significantly affect β-cell tumorigenesis in RT2 mice (Suppl. Figure S3E,F).

Taken together, the data show that high levels of Lhx2 expression are sufficient to promote mammary tumor growth, tumor cell intravasation and metastasis formation, while the genetic ablation of Lhx2 expression only reduces tumor cell intravasation, yet does not affect primary tumor growth and metastatic incidence. Hence, additional molecular pathways may exist that compensate for Lhx2 function.

3.3. *Lhx2 enhances vessel maturation and functionality*

To assess the cell-autonomous effects of Lhx2 expression, we derived primary cell lines from tumors of MPY, MPY;MLhx2 and MPY;MCre;Lhx2$^{fl/fl}$ (MPY;Lhx2KO) mice. *In vitro* proliferation assays showed that neither Lhx2 overexpression nor Lhx2 ablation affected the growth rate of these cells (Suppl. Figure S4A,B), suggesting that the increased growth of primary tumors in MPY;MLhx2 mice is a result of a cross-talk between tumor cells and the tumor microenvironment. We thus investigated the microvascular densities of the different genotype tumors and the maturation and functionality of their tumor vasculature. Immunofluorescence staining of tumor sections with antibodies against the endothelial marker CD31 revealed significantly reduced vessel densities and highly dilated vessels in tumors of MPY;MLhx2 and MN;MLhx2 mice as compared to MPY and MN littermates (Figure 4A,B).

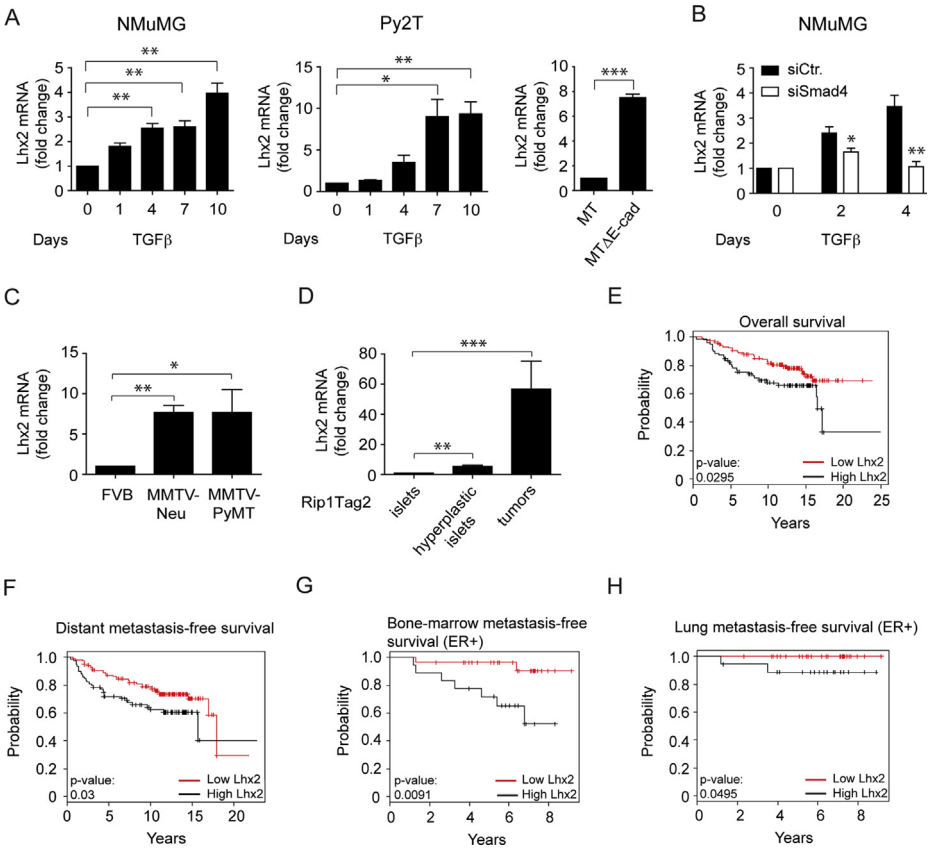

Figure 1 – Lhx2 expression is induced during an EMT, and its high expression levels correlate with poor prognosis in breast cancer patients. A. Quantitative RT-PCR analysis of Lhx2 mRNA levels in NMuMG cells and in Py2T cells induced to undergo EMT by TGFβ-treatment for the days indicated, and in epithelial MT and mesenchymal MTE-cad cells. Shown are the fold-changes as compared to day 0 (no TGFβ) or epithelial MT cells ($n = 3$, $^{**}p < 0.01$ Student's *t*-test). B. Lhx2 mRNA levels were determined by quantitative RT-PCR in NMuMG cells transiently transfected with siRNA against Smad4 (siSmad4) or with control siRNA (siCtr) and treated for four days with TGFβ ($n = 3$, $^{*}p < 0.05$, $^{**}p < 0.01$, $^{***}p < 0.001$ Student's *t*-test). C. Lhx2 mRNA levels were determined by quantitative RT-PCR in mammary glands of normal FVB/N mice and in tumors of MMTV-Neu and MMTV-PyMT transgenic mice ($n = 5$, $^{*}p < 0.05$, $^{**}p < 0.01$ Mann-Whitney test). D. Lhx2 mRNA levels were measured by quantitative RT-PCR in normal islets of Langerhans and in hyperplastic islets and tumors of Rip1Tag2 transgenic mice ($n = 5$, $^{***}p < 0.001$ Mann–Whitney test). E–H. Kaplan–Meier survival analysis revealed significant correlation between high Lhx2 expression levels and poor overall survival (E) and distant-metastasis free survival (F) in breast cancer patients (TRANSBIG database). Kaplan–Meier survival analysis also showed a significant correlation between high Lhx2 expression and low bone-marrow metastasis free survival (G) and lung metastasis free survival (H) in ER+ breast cancer patients (Minn database).

Vessel maturation and functionality are critical vascular parameters influencing tumor growth (Furuhashi et al., 2004; Mazzone et al., 2009; Cheng et al., 2013). Therefore, we co-stained tumor sections against CD31 and the pericyte marker NG2 and determined vessel maturation as the percentage of $NG2^+$ per $CD31^+$ blood vessels. Tumors of both MPY;MLhx2 and MN;MLhx2 mice revealed significantly increased subsets of $NG2^+/CD31^+$ vessels as compared to MPY and MN tumors (Figure 4A,B). To assess whether this vessel maturation coincided with vessel functionality, mice were perfused with fluorescence-labeled lectin prior sacrifice. MPY;MLhx2 tumors contained a significantly higher number of lectin-perfused vessels (80 ± 2%) compared to MPY control tumors (30 ± 3%) (Figure 4C). Consistent with the functionality of the vessels, tumors of MPY;MLhx2 mice exhibited significantly less hypoxia (2 ± 0.1%) as compared to MPY single-transgenic mice (12 ± 1.5%) (Figure 4D). In both genotype tumors, hypoxia was never detected in the vicinity of lectin-perfused blood vessels (Figure 4E). Moreover, approximately 80% of $NG2^+$ vessels were lectin-positive in both MPY;MLhx2 and MPY tumors (Figure 4F), underscoring the functional connection between vessel maturation, vessel functionality and oxygen delivery. Tumors of MPY;MCre;$Lhx2^{fl/fl}$ mice did not show any difference in vessel morphology, density or maturation (Suppl. Figure S4C). In tumors of RT2;RCre; $Lhx2^{fl/fl}$ mice vessel density was increased, yet no alteration in vessel maturation was observed (Suppl. Figure S4D). Together the data indicate that transgenic expression of the transcription factor Lhx2 supports blood vessel maturation, vessel functionality and oxygen delivery.

3.4. *Lhx2 promotes tumor cell migration and invasion*

Lhx2 is induced during EMT in both normal (NMuMG) and transformed mammary epithelial cells (Py2T and MTΔE-cad; Figure 1A). To address the cell-autonomous role of Lhx2 during EMT, we further isolated primary tumor cell clones from MPY;MLhx2-overexpressing tumors (MPY;MLhx2 #965 and #983) and from Lhx2-depleted tumors of MPY;MCre;$Lhx2^{fl/fl}$ mice (MPY;MLhx2KO #791 and #794). The efficiency of Lhx2

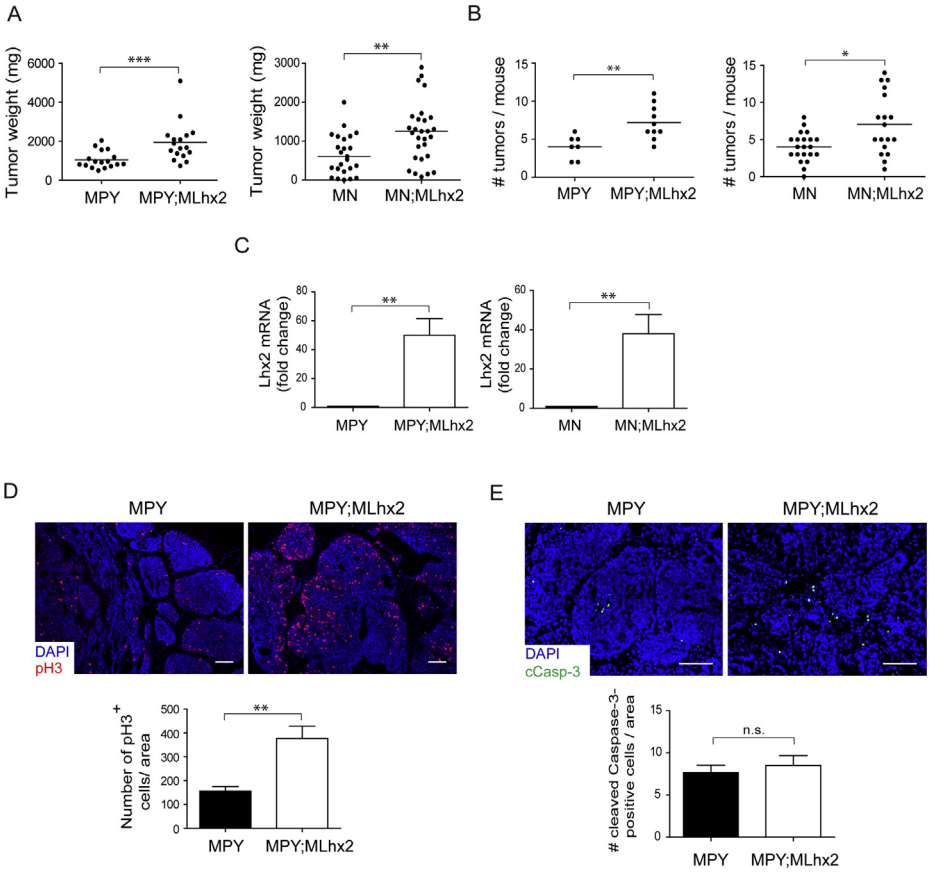

Figure 2 – Lhx2 overexpression enhances mouse mammary tumor growth. A. Tumor weights of 12 week old MPY;MLhx2, MN;MLhx2 and MPY, MN littermate control mice. Each data point represents one mouse ($p < 0.01$, ***$p < 0.001$ Mann–Whitney test). B. Tumor incidences of 12 week old MPY;MLhx2, MN;MLhx2 and MPY, MN littermate control mice. Each data point represents one mouse (*$p < 0.05$, **$p < 0.01$ Mann–Whitney test). C. Lhx2 mRNA levels were determined by quantitative RT-PCR in tumors of 12 week old MPY;MLhx2, MN;MLhx2 and MPY, MN littermate control mice ($n = 3$, **$p < 0.01$ Mann–Whitney test). D. The proliferation rates in tumors of MPY;MLhx2 and MPY control mice were determined by immunofluorescence staining with anti-phospho-histone-3 (pH3) antibody. Numbers of pH3-positive cells per DAPI area are indicated ($n = 5$, **$p < 0.01$ Mann–Whitney test). Scale bars = 100 μm. E. Apoptotic cells were visualized by immunofluorescence staining with antibodies against cleaved caspase-3 (green) in tumors of MPY;MLhx2 and their respective littermate MPY controls. Numbers of cleaved caspase-3-positive cells per DAPI area were determined ($n = 5$).**

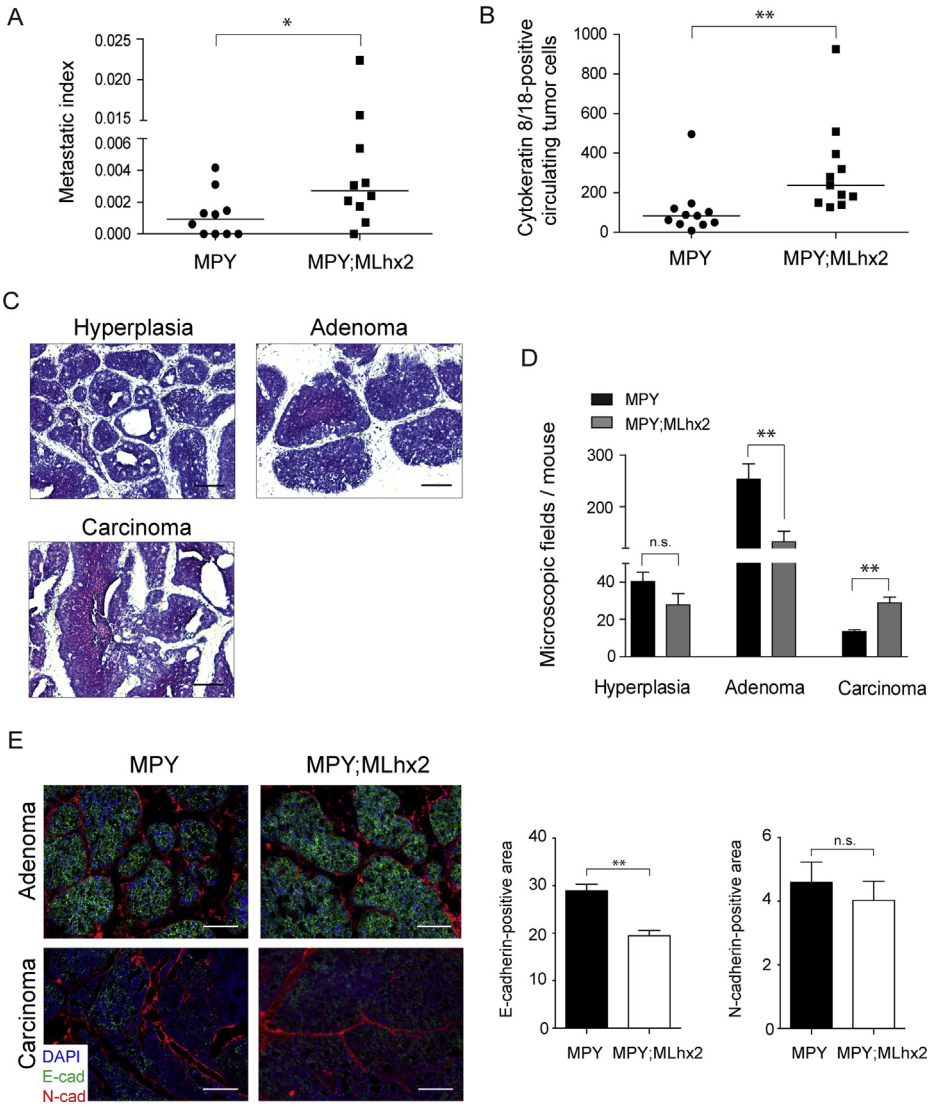

Figure 3 – Lhx2 promotes tumor cell intravasation and metastasis. A. Lung metastasis in MPY;MLhx2 and MPY control mice were detected by H&E staining. The metastatic index was determined as number of lung metastasis divided by primary tumor weight (mg) in each individual mouse (*$p < 0.05$ Mann–Whitney test). B. Average numbers of circulating tumor cells in the peripheral blood of MPY;MLhx2 and MPY littermate control mice are displayed ($p < 0.01$ Mann–Whitney test). C. Histological sections of MPY mice exemplifying the grading stages (hyperplasia, adenoma and carcinoma) of tumors in MPY;MLhx2and MPY mice are shown. Scale bar = 100 μm. D. The incidence of tumor grades (hyperplasia, adenoma and carcinoma) in MPY;MLhx2 and MPY control mice are shown as number of microscopic fields of tumor sections per mouse for the particular grading stages (10 mice for each genotype). E. Immunofluorescence microscopy analysis of changes in the localization and expression levels of the EMT markers E-cadherin (green) and N-cadherin (red) in tumor sections from MPY;MLhx2 and the respective MPY littermate control mice. E-cadherin and N-cadherin positive area per DAPI area were calculated ($n = 5$, **$p < 0.01$ Mann–Whitney test). Scale bar = 100 μm.**

overexpression and silencing and the genotype of the cell lines were verified by immunoblotting and PCR analysis, respectively (Suppl. Figure S5A,B). Primary tumor cell lines isolated from tumors of MPY single-transgenic mice were used as controls (MPY #967 and #844) (Suppl. Figure S5A,B).

Immunofluorescence staining revealed low levels of Lhx2 localization in the nucleus of MPY cells (Suppl. Figure S5C). MPY;MLhx2 cells displayed both nuclear and cytoplasmic distribution of Lhx2, and a comparable localization of endogenous Lhx2 at lower amounts was observed in MPY cells treated with TGFβ for ten days. As expected, Lhx2 was undetectable in MPY;MLhx2KO cells (Suppl. Figure S5C). Immunoblotting confirmed the induction of Lhx2 expression by treatment of MPY cells with TGFβ for ten days and the complete lack of Lhx2 expression in MPY;MLhx2KO cells (Suppl. Figure S5D). These cell lines were used in transwell migration and Matrigel invasion assays to assess whether Lhx2 expression affects cell migration and invasion. Forced expression of Lhx2 in MPY;MLhx2 cells showed a significant increase of both cell migration and invasion (Figure 5A). Similar results were observed in Py2T cells and MT cells forced to express Lhx2 by stable transfection (Py2T-Lhx2 and MT-Lhx2 cells)

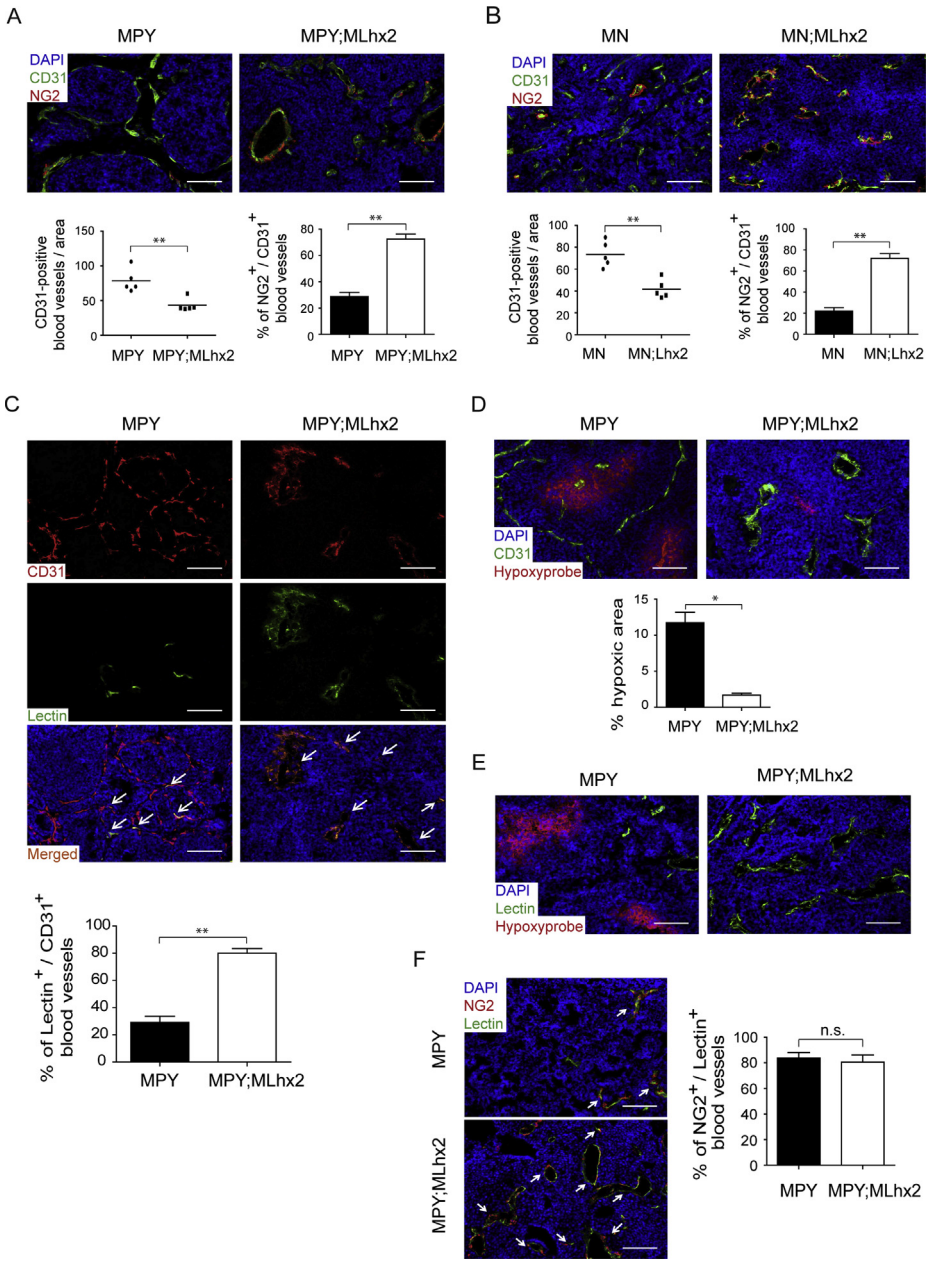

Figure 4 – Lhx2 promotes tumor vessel maturation and functionality. A, B. Immunofluorescence staining with antibodies against CD31 (endothelial cells; green) and against NG2 (pericytes; red) on tumor sections of MPY;MLhx2 (A), MN;MLhx2(B) and MPY, MN littermate control mice are shown. Scale bar = 100 μm. Numbers of blood vessels per DAPI area were calculated. Each data point represents data from a single mouse. Vessel maturation was determined as percentage of NG2-positive per CD31-positive vessels ($n = 5$, $^{**}p < 0.01$ Mann–Whitney test). C. Immunofluorescence staining with antibodies against CD31 (red) on tumor sections from MPY;MLhx2 and control MPY mice previously perfused with FITC-lectin (green). Scale bar = 100 μm. Vessel perfusion was quantified as the percentage of FITC-lectin perfused vessels of the total number of CD31-positive blood vessels per analyzed tumor area ($n = 5$, $^{**}p < 0.01$ Mann–Whitney test). D. Sections of MPY;MLhx2 and control tumors were stained for CD31 (green) and hypoxyprobe (red) and the percentages of hypoxic area per DAPI area were determined ($n = 5$, $^{*}p < 0.05$ Mann–Whitney test). Scale bar = 100 μm. E. Immunofluorescence micrographs of tumor sections of FITC-lectin-perfused (green) MPY;MLhx2 and MPY control mice stained with antibodies against hypoxyprobe (red) are shown ($n = 5$). Scale bar = 100 μm. F. Tumor sections from FITC-lectin-perfused (green) MPY;MLhx2 and MPY control mice were co-stained with antibodies against NG2 (red). Arrows indicate areas of NG2/lectin co-localization. Scale bar = 100 μm. Percentages of NG2-positive per lectin-positive blood vessels are indicated ($n = 5$).

(Figure 5B,C). In NMuMG cells constitutively overexpressing Lhx2, only migration was increased (Suppl. Figure S5E); these cells did not invade in Matrigel. Cell proliferation assays revealed no alteration between MPY;MLhx2, Py2T-Lhx2 and MT-Lhx2 cells and their corresponding control cells (Suppl. Figure S5F–H).

Converse to Lhx2 overexpression, depletion of Lhx2 revealed a significant reduction of both migration and

invasion of MPY;MLhx2KO cells (Figure 5D), in Py2T cells transiently expression siRNAs against Lhx2 (treated for ten days with TGFβ) (Figure 5E) and in MTΔE-cad cells stably expressing shRNAs against Lhx2 (Figure 5F). In NMuMG cells silenced for Lhx2 and treated for ten days with TGFβ, migration was significantly decreased (Suppl. Figure S6A). Loss of Lhx2 expression did not affect cell proliferation of MPY cells (Suppl. Figure S6B). In addition, Annexin-V staining showed no difference in the extent of apoptosis between Py2T-siLhx2, MTΔE-cad-shLhx2 and NMuMG-siLhx2 and siControl-transfected cells (Suppl. Figure S6C).

The fact that Lhx2 regulates tumor cell migration and invasion motivated us to investigate the functional contribution of Lhx2 to an EMT. In contrast to the epithelial morphology of MPY cells, Lhx2-expressing MPY;MLhx2 tumor cells exhibited an elongated, mesenchymal-like morphology (Figure 6A). However, when compared to MPY cells treated for ten days with TGFβ, MPY;MLhx2 cells were not as elongated. Immunofluorescence microscopy analysis for various EMT markers demonstrated a critical role for Lhx2 in EMT. Similar to MPY cells induced to undergo an EMT by TGFβ treatment, the forced expression of Lhx2 in MPY;MLhx2 tumor cells led to a loss of E-cadherin and ZO1 expression and localization at the cell membranes (Figure 6A). Conversely, expression of the mesenchymal markers N-cadherin and vimentin was induced in MPY;MLhx2 cells, similar to their expression in TGFβ-treated MPY cells (Figure 6A). Comparable results were obtained in Py2T-Lhx2 cells (Suppl. Figure S7A,B), suggesting that Lhx2 overexpression induces a cadherin switch and at least a partial EMT.

We next analyzed whether Lhx2 is critically required for an EMT to occur. MPY;MLhx2KO and control cells were treated for ten days with TGFβ to undergo an EMT. Even though we did not observe changes in cell morphology, immunofluorescence staining for EMT markers revealed a maintenance of E-cadherin and ZO1 expression and a failure to induce the expression of the mesenchymal markers N-cadherin and vimentin in TGFβ-treated MPY;Lhx2KO cells as compared to TGFβ-treated MPY cells (Figure 6B). These data were confirmed in Py2T-siLhx2 cells transiently knock-down for Lhx2 (Suppl. Figure S7C,D).

A pro-invasive function of Lhx2 was further observed in 3D Matrigel cultures. While epithelial Py2T and MT cells grew as epithelial spheres, TGFβ-treated Py2T cells and MTΔE-cad mesenchymal cells showed substantial invasion into Matrigel (Figure 6C,D). Notably, siRNA and shRNA-mediated depletion of Lhx2 expression in the mesenchymal cells repressed cell invasion and reinstalled the epithelial growth pattern. These results indicate that Lhx2 is able to induce cell migration and invasion and exerts critical functions during an EMT.

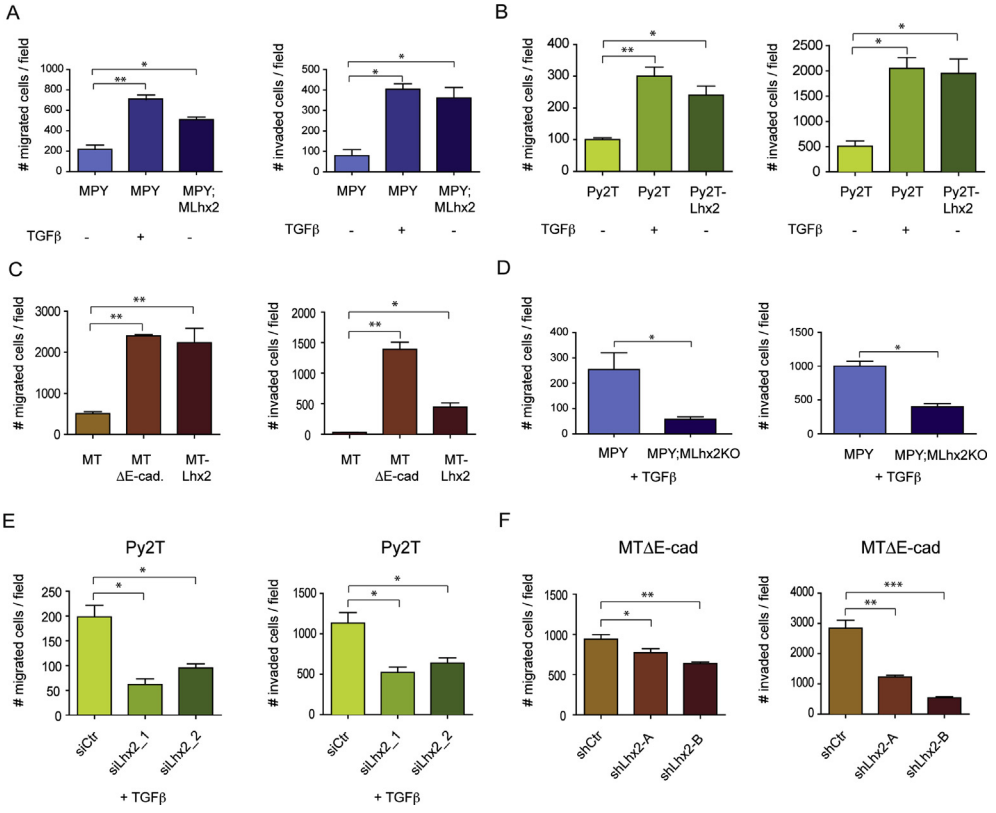

Figure 5 – Lhx2 promotes mammary tumor cell migration and invasion. A–F. Lhx2-overexpressing cells or cells depleted in Lhx2 expression and their respective control cells were seeded into migration or invasion Boyden chambers in the absence or presence of TGFβ and allowed to pass through the membrane pores for 24 h along an FBS gradient. Cells that passed through the membrane pores were stained with DAPI and then counted ($n = 3$, $^{*}p < 0.05$, $^{**}p < 0.01$, $^{***}p < 0.001$ Student's t-test): (A) MPY:Lhx2 and MPY; (B) Py2T-Lhx2 and Py2T; (C) MT-Lhx2, MT and MTΔE-cad; (D) MPY;MLhx2KO and MPY; (E) Py2T-siLhx2_1, Py2T-siLhx2_2 and Py2T-siCtr; (F) MTΔE-cad-shLhx2_A, MTΔE-cad-shLhx2_B and MTΔE-cad-siCtr.

3.5. *Lhx2 regulates tumor cell migration and invasion via PDGF-B/PDGFRβ signaling*

The PDGF-B/PDGFRβ signaling pathway has been previously shown to stimulate cell migration and invasion in a variety of non-transformed and transformed cell types (Koyama et al., 1994; Thommen et al., 1997; Yu et al., 2001; ten Freyhaus et al., 2006; Abouantoun and MacDonald, 2009). Moreover, PDGFR signaling has been shown to play a critical role during EMT and the metastatic process (Jechlinger et al., 2006). The expression of PDGF-A and B and PDGFRβ was also found substantially upregulated during TGFβ-induced EMT in NMuMG cells (Lehembre et al., 2008). Hence, by using quantitative RT-PCR and immunoblotting we examined the expression of the respective PDGF ligands and receptors in both Lhx-2 overexpressing and Lhx2-silenced primary tumor cells. PDGF-B expression was increased in MPY;MLhx2 and decreased in MPY;Lhx2KO cells (Figure 7A and Suppl. Figure S8A–C). This effect was independent of TGFβ. Of the PDGFR family members, ten days of TGFβ treatment induced only PDGFRβ protein and mRNA expression in an Lhx2-independent manner (Figure 7A and Suppl. Figure S8C). PDGFRβ expression did not require canonical TGFβ signaling, since siRNA-mediated ablation of Smad4 had no effect on TGFβ-induced PDGFRβ expression (Suppl. Figure S8D). The data indicate that PDGF-B expression is induced during EMT

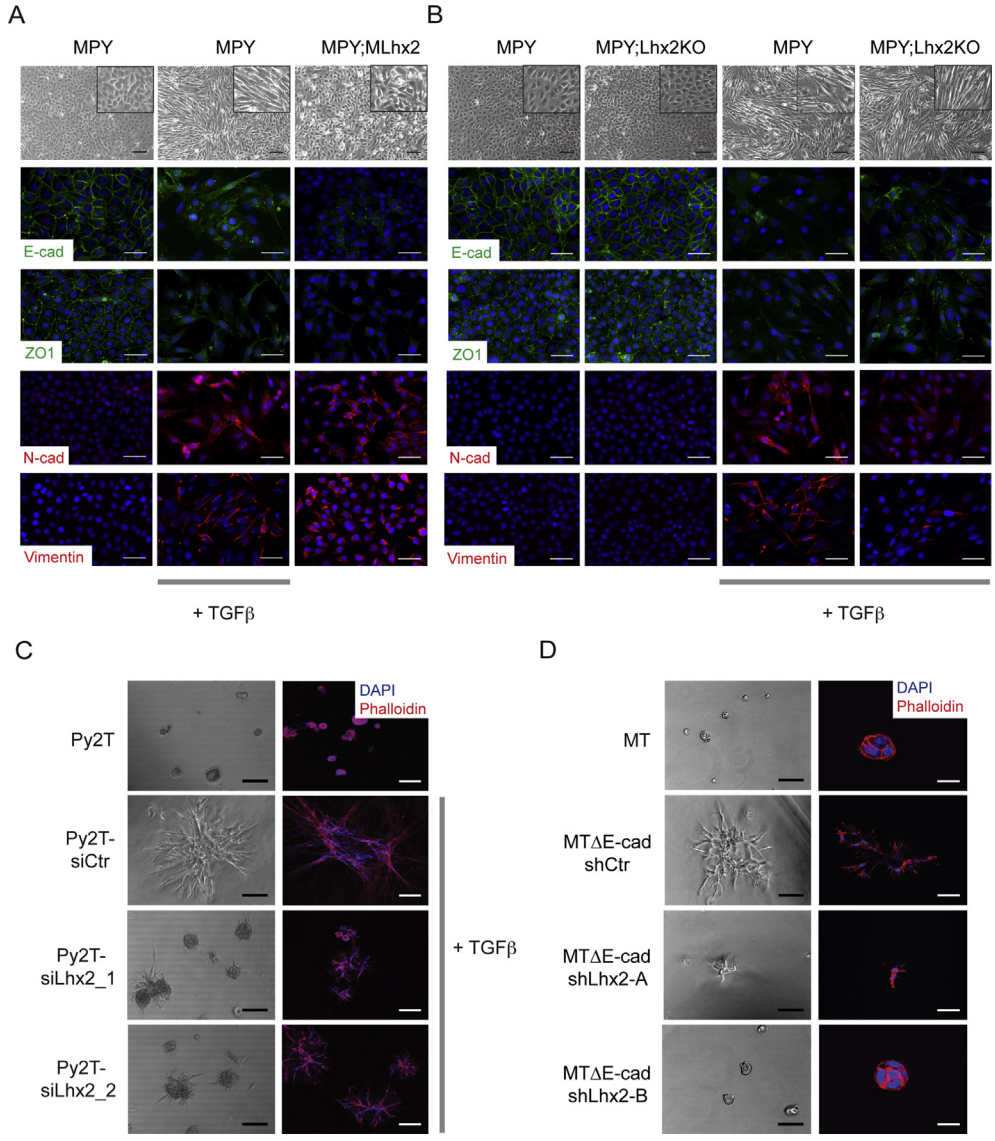

Figure 6 – Lhx2 promotes EMT. A, B. Analysis of EMT marker expression in MPY;MLhx2 and MPY control cells (A) and MPY;MLhx2KO and MPY control cells (B) in the absence or presence of TGFβ as indicated. Phase contrast microscopy images and immunofluorescence staining with antibodies against E-cadherin and ZO1 (epithelial markers) and N-cadherin and vimentin (mesenchymal markers) are shown. Scale bars = 50 μm. C, D. Untreated Py2T cells or Py2T cells transiently transfected with siRNAs against Lhx2 (Py2T-siLhx2_1, Py2T-siLhx2_2) or control siRNA (Py2T-siCtr) in the absence or presence of TGFβ (C) and MTΔE-cad cells stably expressing shRNAsaginst Lhx2 (MTΔE-cad-shLhx2_A, MTΔE-cad-shLhx2_B) or control shRNA (MTΔE-cad-shCtr) and untreated MT cells (D) were grown in three-dimensional Matrigel, and analyzed by phase contrast microscopy and by phalloidin (red) and DAPI (blue) immunofluorescence staining. Scale bars = 50 μm.

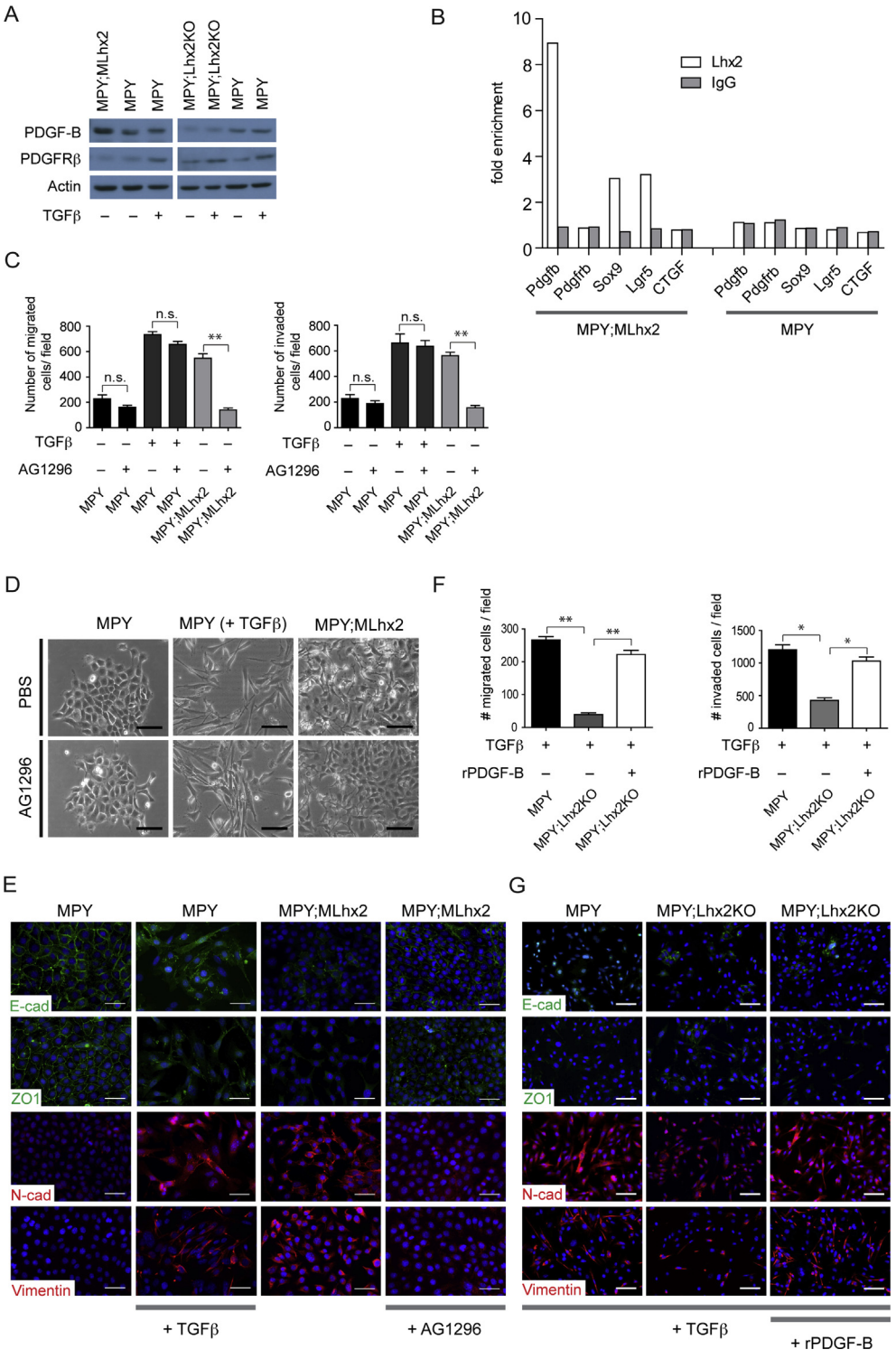

Figure 7 – Lhx2 induces tumor cell migration and invasion via PDGF-B/PDGFRβ signaling. A. Immunoblotting analysis of PDGF-B and PDGFRβ in lysates of MPY;MLhx2, MPY;MLhx2KO and MPY control cells in the presence and absence of TGFβ as indicated. Immunoblotting against actin was used as loading control. B. Chromatin immunoprecipitation of MPY;MLhx2 cells treated with antibodies against Lhx2. Precipitated DNA fragments corresponding to *Pdgfb* promoter sequences were detected by quantitative PCR to assess Lhx2 occupancy at this region. Fold changes are shown in comparison to a PCR reaction with primers specific for an intergenic region. ChIP of promoter sequences of the known Lhx2 target genes *Sox9* and *Lgr5* were used as positive controls and *CTGF1a1b* gene served as negative control. C. Boyden chamber migration and invasion assays were performed on MPY;MLhx2 and MPY control cells treated for 24 h with the PDGFRβ inhibitor AG1296 and with TGFβ as indicated ($n = 3$, $^{**}p < 0.01$ Student's *t*-test). D. Phase contrast micrographs of MPY;MLhx2 and MPY control cells treated with AG1296 and TGFβ as indicated. Scale bar = 50 μm. E. Expression of the EMT markers E-cadherin, ZO1, N-cadherin and vimentin were analyzed by immunofluorescence microscopy with MPY;MLhx2 and MPY control cells treated with AG1296 or TGFβ as indicated. Scale

in an Lhx2-dependent manner, while PDGFRβ expression is upregulated independent of Lhx2 and canonical TGFβ signaling. Quantification of PDGF-B levels by ELISA revealed a significant increase of PDGF-B protein in MPY;MLhx2 cells supernatant compared to MPY;Lhx2KO and MPY control cells, while PDGF-B protein levels were significantly reduced in supernatants of MPY;Lhx2KO cells (Suppl. Figure S8E).

To test whether the *Pdgfb* gene is a direct transcriptional target of Lhx2, we performed chromatin immunoprecipitation (ChIP) followed by quantitative PCR to determine whether Lhx2 can directly bind the *Pdgfb* gene promoter. Indeed, ChIP with antibodies against Lhx2 in MPY;MLhx2 cells resulted in the precipitation of promoter sequences of *Pdgfb* but not of *Pdgfrb* (Figure 7B). The known Lhx2 target genes *Sox9* and *Lgr5* were used as positive controls (Mardaryev et al., 2011) and the *CTGF1a1b* promoter as negative control. Comparable results were found in NMuMG cells induced to undergo EMT and to upregulate Lhx2 expression by the presence of TGFβ (Suppl. Figure S8F). In addition, gene expression profiling analysis performed on NMuMG cells stably expressing Lhx2 or transiently depleted in Lhx2 expression revealed increased and decreased PDGF-B mRNA expression, respectively (Suppl. Table). These data indicate that Lhx2 directly regulates the expression of the *Pdgfb* but not of the *Pdgfrb* gene.

To test the hypothesis that Lhx2 regulates cell migration and invasion during an EMT by inducing PDGF-B expression, we treated MPY;MLhx2 cells for 24 h with the PDGFRβ tyrosine kinase inhibitor AG1296. Both cell migration and invasion were significantly reduced in MPY;MLhx2 cells treated with AG-1296 as compared to control-treated MPY;MLhx2 cells (Figure 7C). It is noteworthy that AG1296 did not reduce cell migration of TGFβ-treated MPY cells, suggesting that, in addition to the Lhx2-mediated expression of PDGF-B, other pathways are activated during TGFβ-induced EMT that promote cell migration. Cell proliferation was not affected by PDGFRβ activity repression (Suppl. Figure S9A). Immunoblotting analysis confirmed the inhibition of PDGFRβ phosphorylation by AG1296 (Suppl. Figure S9B). Phase contrast microscopy revealed that MPY;MLhx2 cells treated with AG1296 exhibited a more epithelial-like phenotype as compared to control-treated MPY;MLhx2 cells and to TGFβ-treated MPY cells (Figure 7D). However, AG1296 treatment did not efficiently repress TGFβ-induced EMT in MPY cells, again suggesting that TGFβ may induce other pathways in addition to Lhx2-mediated PDGF-B signaling. Immunofluorescence microscopy analysis confirmed the reversion of the mesenchymal phenotype of MPY;MLhx2 cells into a more epithelial behavior: the epithelial markers E-cadherin and ZO1 displayed increased immunofluorescence staining in AG1296-treated cells, and the mesenchymal markers N-cadherin and vimentin showed decreased expression (Figure 7E).

Notably, addition of recombinant PDGF-B to MPY;Lhx2KO cells reinstalled TGFβ-induced cell migration and invasion that had been lost by the genetic ablation of Lhx2 (Figure 7F) without affecting cell proliferation (Suppl. Figure S9C). Recombinant PDGF-B also led to an activation of PDGFRβ, as indicated by increased phosphorylation of PDGFRβ (Suppl. Figure S9D). While E-cadherin and ZO-1 expression and localization was not substantially affected by recombinant PDGF-B, the mesenchymal markers N-cadherin and vimentin showed increased expression in recombinant PDGF-B-treated cells (Figure 7G).

In conclusion, the results indicate that Lhx2 promotes tumor cell migration and invasion by directly inducing PDGF-B expression and by stimulating PDGF-B/PDGFRβ signaling.

3.6. *PDGF-B/PDGFRβ signaling is required for Lhx2-mediated tumor growth and metastasis*

We next assessed whether Lhx2-mediated PDGF-B expression also played a role in Lhx2-mediated tumor growth and metastasis formation. Immunostaining of histological tumor sections revealed high expression of PDGF-B by MPY;MLhx2 tumor cells and decreased levels in MPY;Lhx2KO tumor cells as compared to MPY controls (Suppl. Figure S10A). As reported by previous studies (Sugimoto et al., 2006; Cooke et al., 2012), PDGFRβ was found mainly localized on $NG2^{+}$pericytes (Suppl. Figure S10B).

Previously, PDGF-B expression by tumor cells has been associated with increased pericyte abundance and increased tumor growth (Abramsson et al., 2003; Guo et al., 2003; Furuhashi et al., 2004) and with vessel maturation and perfusion of tumor vessels (Mazzone et al., 2009). We thus examined whether PDGF-B/PDGFRβ signaling is responsible for the increased blood vessel maturation and functionality (Figure 4A,C) and for the accelerated tumor growth and malignancy found with MPY;MLhx2 tumors (Figures 2A and 3A). MPY and MPY;MLhx2 mice were treated for 21 days with Imatinib, an inhibitor of PDGFRβ and also of the tyrosine kinase activities of BCR-Abl and c-Kit. In comparison to PBS placebo control, Imatinib significantly reduced tumor growth in MPY;MLhx2 double-transgenic mice, while tumor growth in single-transgenic MPY mice remained unaffected (Figure 8A). Staining of tumor sections for pH3 revealed a decrease in proliferating cells in Lhx2-overexpressing tumors treated with Imatinib (Suppl. Figure S10C). Cleaved caspase-3 staining of tumor sections showed no alteration in the rates of apoptosis between the groups (Suppl. Figure S10D). Immunofluorescence staining against CD31 revealed increased numbers of blood vessels in Imatinib-treated as compared to PBS-treated MPY;MLhx2 mice, and the percentage of NG2+ mature vessels was significantly lower in the Imatinib-treated MPY;MLhx2 group (Figure 8B). Furthermore, lectin perfusion experiments showed a significant reduction of perfused vessels in the Imatinib-treated MPY;MLhx2 tumors, accompanied by a significant increase in tissue hypoxia (Figure 8C and D) and VEGF-A mRNA expression (Suppl. Figure S10E). Hypoxia was never found in close vicinity of

bar = 50 μm. F. Boyden chamber migration and invasion assays were performed on MPY;Lhx2KO and MPY control cells treated with TGFβ for ten days and with recombinant (r)PDGF-B for 48 hours ($n = 3$, $^{*}p < 0.05$,$^{**}p < 0.01$ Student's *t*-test). G. Immunofluorescence microscopy analysis was performed for the expression of E-cadherin, ZO1, N-cadherin and vimentin on MPY;Lhx2KO and MPY control cells treated with recombinant (r)PDGF-B and TGFβ as indicated. Scale bar = 50 μm.

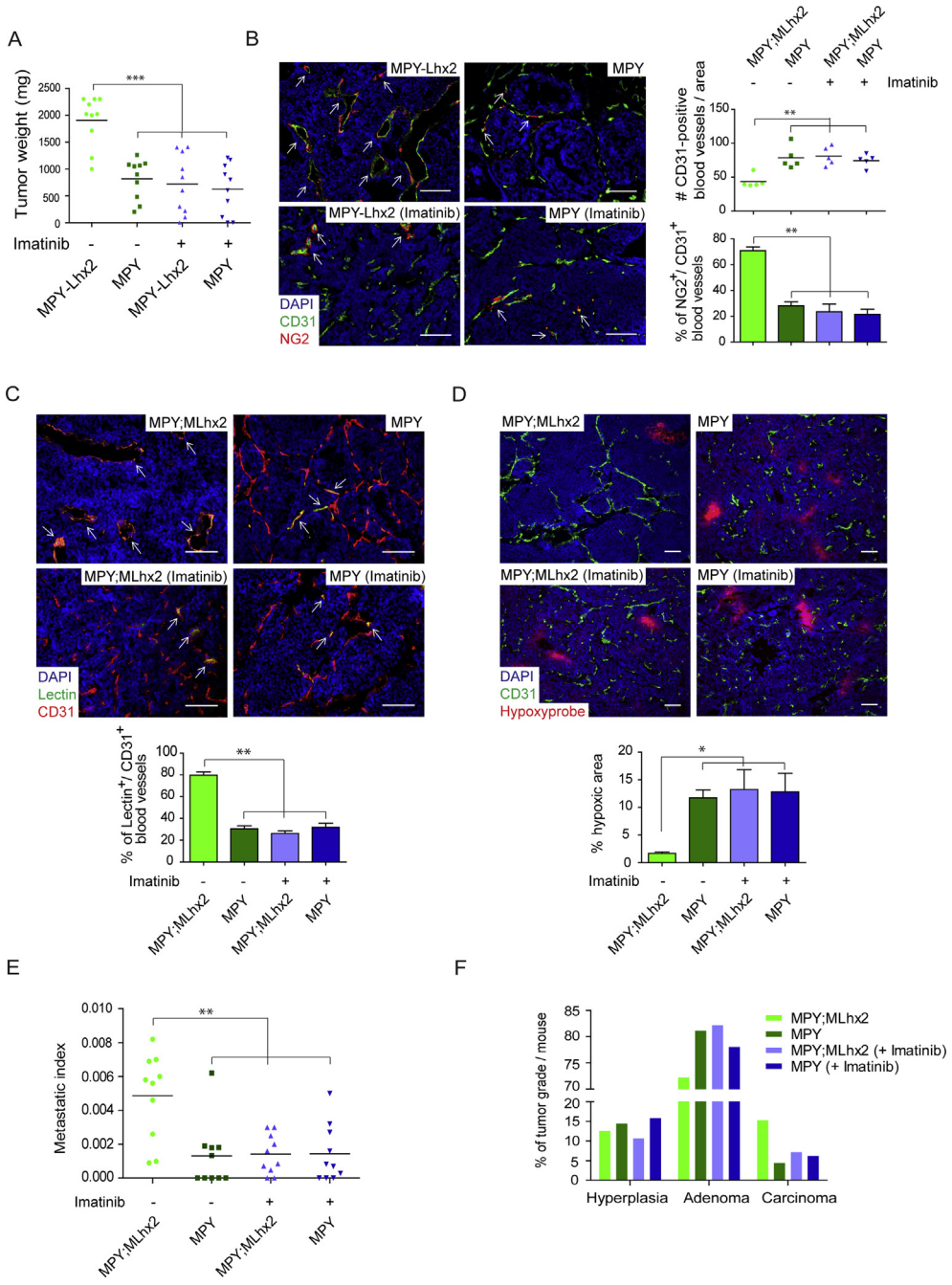

Figure 8 – PDGF-B/PDGFRβ signaling is required for Lhx2-mediated tumor growth and metastasis. A. MPY;MLhx2 and MPY mice were treated for 21 days with Imatinib or PBS-vehicle and sacrificed at the age of 12 weeks. Tumor weights (mg) were measured and plotted as cumulative data points from each individual mouse (* $p < 0.001$ Mann–Whitney test). B. Immunofluorescence staining for CD31 (green) and NG2 (red) of tumor sections of MPY;MLhx2 and MPY mice that have been treated with Imatinib or PBS control. Arrows indicate sites of co-localization. Scale bar = 100 μm. Numbers of blood vessels and the percentages of mature vessels are indicated ($n = 5$, ** $p < 0.01$ Mann–Whitney test). C. Vessel functionality was assessed by immunofluorescence staining with CD31 (red) on tumor sections of FITC-lectin perfused (green) MPY;MLhx2 and MPY mice treated with Imatinib or PBS. Arrows indicate sites of co-localization. Scale bar = 100 μm. Vessel perfusion was quantified as described in Figure 4C ($n = 5$, ** $p < 0.01$ Mann–Whitney test). D. Sections of tumors of MPY;MLhx2 and MPY mice treated with Imatinib or PBS were stained for CD31 (green) and hypoxyprobe (red), and the hypoxic area was determined as described in Figure 4D ($n = 5$, * $p < 0.05$ Mann–Whitney test). Scale bar = 100 μm. E. Metastasis in lungs of MPY;MLhx2 and MPY mice treated with Imatinib or PBS were detected by H&E staining of lung sections. The metastatic index was calculated as described in Figure 3A ($n = 10$, ** $p < 0.01$ Mann–Whitney test). F. Percentages of tumor grades (hyperplasia, adenoma and carcinoma) per MPY;MLhx2 and MPY mouse treated with Imatinib or PBS are displayed ($n = 10$).**

lectin-perfused vessels in all experimental groups (Suppl. Figure S10F), underscoring the importance of vessel functionality for oxygen delivery.

We next analyzed the effects of the inhibition of PDGFRβ-signaling on metastasis formation. MPY;MLhx2 tumor-bearing mice treated with Imatinib displayed significantly less lung metastasis as compared to PBS-treated MPY;MLhx2 mice (Figure 8E). In addition, tumor grading revealed a decreased incidence of carcinomas and an increased incidence of adenomas in MPY;MLhx2 tumors treated with Imatinib as compared to tumors of PBS-treated MPY;MLhx2 mice (Figure 8F). No difference in lung metastasis and tumor staging was observed between Imatinib and PBS-treated MPY tumors (Figure 8E and F).

Together, the data indicate that, by directly inducing *Pdgfb* gene expression, Lhx2 mediates autocrine and paracrine PDGF-B/PDGFRβ signaling and promotes an EMT and tumor invasion and blood vessel maturation and functionality, respectively. Both pathways cooperate to accelerate primary tumor growth and to promote malignant tumor progression and metastasis formation.

4. Discussion

Hallmarks of EMT are frequently observed at the invasive front of various solid tumors (Brabletz et al., 2005; Huber et al., 2005; Christofori, 2006; Thiery and Sleeman, 2006; Trimboli et al., 2008; Usami et al., 2008; Vergara et al., 2010). Here, we have identified the transcription factor Lhx2 as a critical factor during EMT in both normal murine mouse mammary cells (NMuMG) and in murine breast cancer cell lines (Py2T, MTΔE-cad, MPY). Elevated expression of Lhx2 is also found in a variety of human malignancies (Breast Cancer Database, http://www.itb.cnr.it/breastcancer/php/geneReport.php?id=9355) (Gorantla et al., 2011) and correlates with poor prognosis of breast cancer patients (this work). However, the functional role of Lhx2 during EMT, tumor progression and metastasis has remained elusive.

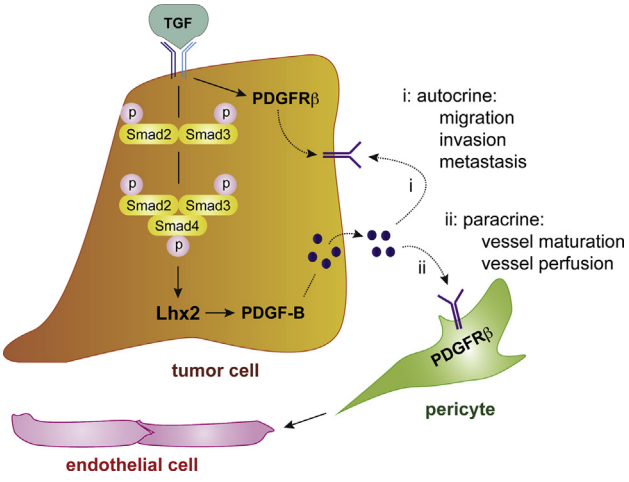

Figure 9 – A working model of Lhx2-induced tumor progression. Canonical TGFβ signaling induces the expression of Lhx2 in tumor cells. Concomitantly, PDGFRβ expression in tumor cells is upregulated independently of Lhx2 by non-canonical TGFβ signaling. Lhx2 directly induces expression of PDGF-B which in turn activates PDGFRβ signaling via two mechanisms: (i) tumor cell-produced PDGF-B binds to PDGFRβ on tumor cells and promotes tumor cell migration and invasion in an autocrine signaling pathway and (ii) PDGF-B binds PDGFRβ expressed on pericytes in a paracrine manner and promotes blood vessel maturation and functionality leading ultimately to an improved delivery of oxygen and nutrients and thus to increased tumor growth.

We show that the expression of Lhx2 is induced by canonical TGFβ signaling. Gain and loss of function experiments in cultured cell lines reveal that Lhx2 exerts a critical role in EMT and tumor progression. Forced expression of Lhx2 induces partial EMT and cell migration and invasion in normal mammary epithelial cells and in breast cancer cells. Conversely, the genetic ablation of Lhx2 expression leads to a delay in EMT and reduced cell migration and invasion.

We also report elevated Lhx2 expression during multistage carcinogenesis in the MMTV-PyMT (MPY) and MMTV-Neu (MN) transgenic mouse models of breast cancer and in the Rip1Tag2 (RT2) transgenic mouse model of pancreatic β-cell carcinogenesis. Transgenic expression of Lhx2 in mammary epithelial cells does not lead to any mammary gland abnormalities, indicating that Lhx2 itself is not an oncogene. However, the transgenic expression of Lhx2 in tumor cells of MPY and MN mice leads to faster tumor growth and in MPY mice to increased tumor invasion and to higher numbers of circulating tumor cells and lung metastases. This is accompanied by increased tumor cell proliferation without any effect on tumor cell survival. The increased lung metastasis observed as a consequence of enhanced Lhx2 expression could well be secondary to the concomitant increased proliferation in response to Lhx2 expression. On the other hand, genetic depletion of Lhx2 in tumor cells of MPY and RT2 mice has no major influence on tumor growth and malignant progression. Only the number of circulating tumor cells in the peripheral blood of MPY mice is reduced by the depletion of Lhx2 expression. These data suggest that Lhx2 has the capacity to promote primary tumor growth, tumor invasion and metastasis formation, yet that these functions may be redundant in complex animal models and that it may share its protumorigenic activities with other factors and signaling pathways. The expression levels of Lhx2 by tumor cells may thus be crucial for the outcome of tumor progression. Such dose-dependent effect on tumor growth has been previously reported for other transcription factors (Kuzmanov et al., 2012).

Since the transgenic expression of Lhx2 promotes primary tumor growth *in vivo*, but does not affect cell proliferation *in vitro*, we have investigated how the tumor microenvironment promotes tumor growth *in vivo*. Well-known parameters to influence tumor progression are microvessel density (Weidner et al., 1991) and blood vessel maturation (Furuhashi et al., 2004; Mazzone et al., 2009; Cheng et al., 2013). We find that Lhx2-overexpressing tumors contain less but larger and more dilated vessels. Notably, the majority of these vessels are covered with NG2-positive pericytes, a maturation process required for vessel functionality (Huang et al., 2010; Gibby et al., 2012). Indeed, lectin perfusion experiments demonstrate higher vessel functionality in Lhx2-expressing tumors. Improved vessel perfusion leads to a reduction in

tumor hypoxia and decreased VEGF-A expression, probably the main cause for the diminished angiogenesis observed in Lhx2-overexpressing tumors. Moreover, hypoxia is never observed in the proximity of NG2-positive, mature blood vessels, emphasizing the relevance of vessel maturation for optimal oxygen supply (Gibby et al., 2012). Therefore, we conclude that Lhx2-mediated enhanced vessel maturation leads to improved vessel perfusion, increased oxygen and nutrient delivery, finally resulting in enhanced tumor growth.

PDGF family members are well-known to regulate vessel maturation *in vivo* (Abramsson et al., 2003; Lin et al., 2003; di Tomaso et al., 2009; Kuzmanov et al., 2012). As reported for other mouse models of cancer (Sugimoto et al., 2006; Cooke et al., 2012), PDGFRβ is most profoundly expressed on NG2-positive pericytes. However, we also observe expression of PDGFRβ in cancer cells. Indeed, pharmacological interference with PDGFR-signaling by Imatinib in MPY;MLhx2 mice results in a repression of vessel maturation, vessel perfusion and primary tumor growth.

PDGF family members are also known to play critical roles in cell migration and invasion (Koyama et al., 1994; Thommen et al., 1997; Yu et al., 2001; ten Freyhaus et al., 2006; Abouantoun and MacDonald, 2009). Gain and loss of function experiments in conjunction with gene expression profiling and ChIP analysis demonstrate that Lhx2 directly induces the transcriptional activation of the *Pdgfb* gene. Hence, with the upregulated expression of Lhx2 during EMT and tumor progression, PDGF-B levels are directly increased as well. As reported previously in other cell types (Jechlinger et al., 2003; Boucher et al., 2007), we find that the expression of PDGFRβ, the cognate receptor of PDGF-B, is also induced during EMT, however, in an Lhx2-independent manner. Pharmacological inhibition of Lhx2-induced PDGF-B/PDGFRβ signaling reduces breast cancer cell migration and invasion, while the addition of recombinant PDGF-B rescues cell migration and invasion in cells lacking Lhx2 and thus PDGF-B expression. Hence, *Pdgfb* appears one of the most important target genes of Lhx2 to promote tumor cell migration and invasion. In accordance with our data, PDGF-B/PDGFRβ signaling has been reported as critical for EMT and for human medulloblastoma cell migration and invasion (Jechlinger et al., 2006; Abouantoun and MacDonald, 2009).

In accordance with the critical role of PDGF-B/PDGFRβ signaling in tumor cell migration and invasion *in vitro*, also carcinoma formation in the primary tumor tissue and lung metastasis is repressed in MPY;MLhx2 mice treated with Imatinib. A similar repression of experimental breast tumor progression and metastasis by Imatinib and a correlation of high PDGFRα and β expression in human breast cancers have been reported previously (Jechlinger et al., 2006). However, genetic ablation of Lhx2 expression as well as treatment with Imatinib have no effect on tumor growth and tumor progression in single-transgenic MPY mice, supporting the notion that PDGF-B/PDGFRβ signaling is critical for Lhx2-mediated induction of tumor cell migration and blood vessel maturation, yet that other pathways, independent of Lhx2 and PDGF signaling, may exist.

In conclusion, we demonstrate for the first time a functional contribution of the transcription factor Lhx2 to malignant breast cancer growth and metastasis. By directly inducing transcriptional activity of the *Pdgfb* gene in cancer cells, Lhx2 employs PDGF-B/PDGFRβ signaling for two pro-tumorigenic pathways: (i) in an autocrine loop PDGF-B/PDGFRβ signaling promotes partial EMT, tumor cell migration and invasion, intravasation and metastasis formation, and (ii) in a paracrine manner PDGF-B/PDGFRβ signaling supports blood vessel maturation and functionality and primary tumor growth (Figure 9). The fact that Lhx2 expression shows a significant correlation with clinical outcome of breast cancer patients underscores its relevance in human disease. Finally, the pleiotropic role of Lhx2-induced PDGF-B/PDGFRβ signaling during tumor progression makes it an attractive target for further investigations that potentially may lead to the development of new cancer therapies.

Acknowledgments

We thank Dr. E.S. Monuki (University of California, San Diego, USA) for providing the mouse line carrying LoxP-flanked Lhx2 alleles. We are grateful to U. Schmieder, P. Schmidt, I. Galm, R. Jost and H. Antoniadis for their technical support. This research has been supported by the Swiss National Science Foundation, the Swiss Initiative for Systems Biology (RTD Cell-plasticity), the EU-FP7 framework program TuMIC 2008-201662, the Swiss Cancer League and the Krebsliga Beider Basel.

Appendix A. Supplementary material

Supplementary material related to this article can be found at http://dx.doi.org/10.1016/j.molonc.2013.12.009.

REFERENCES

Abouantoun, T.J., MacDonald, T.J., 2009. Imatinib blocks migration and invasion of medulloblastoma cells by concurrently inhibiting activation of platelet-derived growth factor receptor and transactivation of epidermal growth factor receptor. Mol. Cancer Ther. 8, 1137–1147.

Abramsson, A., Lindblom, P., Betsholtz, C., 2003. Endothelial and nonendothelial sources of PDGF-B regulate pericyte recruitment and influence vascular pattern formation in tumors. J. Clin. Invest. 112, 1142–1151.

Baluk, P., Morikawa, S., Haskell, A., Mancuso, M., McDonald, D.M., 2003. Abnormalities of basement membrane on blood vessels and endothelial sprouts in tumors. Am. J. Pathol. 163, 1801–1815.

Boucher, P., Li, W.P., Matz, R.L., Takayama, Y., Auwerx, J., Anderson, R.G., Herz, J., 2007. LRP1 functions as an atheroprotective integrator of TGFbeta and PDFG signals in the vascular wall: implications for Marfan syndrome. PLoS One 2, e448.

Brabletz, T., Jung, A., Spaderna, S., Hlubek, F., Kirchner, T., 2005. Opinion: migrating cancer stem cells – an integrated concept of malignant tumour progression. Nat. Rev. Cancer 5, 744–749.

Cheng, L., Huang, Z., Zhou, W., Wu, Q., Donnola, S., Liu, J.K., Fang, X., Sloan, A.E., Mao, Y., Lathia, J.D., Min, W., McLendon, R.E., Rich, J.N., Bao, S., 2013. Glioblastoma stem

cells generate vascular pericytes to support vessel function and tumor growth. Cell 153, 139–152.
Chou, S.J., O'Leary, D.D., 2013. Role for Lhx2 in corticogenesis through regulation of progenitor differentiation. Mol. Cell Neurosci. 56C, 1–9.
Christofori, G., 2006. New signals from the invasive front. Nature 441, 444–450.
Cooke, V.G., LeBleu, V.S., Keskin, D., Khan, Z., O'Connell, J.T., Teng, Y., Duncan, M.B., Xie, L., Maeda, G., Vong, S., Sugimoto, H., Rocha, R.M., Damascena, A., Brentani, R.R., Kalluri, R., 2012. Pericyte depletion results in hypoxia-associated epithelial-to-mesenchymal transition and metastasis mediated by met signaling pathway. Cancer Cell 21, 66–81.
Dawid, I.B., Toyama, R., Taira, M., 1995. LIM domain proteins. C R Acad Sci III 318, 295–306.
Desmedt, C., Piette, F., Loi, S., Wang, Y., Lallemand, F., Haibe-Kains, B., Viale, G., Delorenzi, M., Zhang, Y., d'Assignies, M.S., Bergh, J., Lidereau, R., Ellis, P., Harris, A.L., Klijn, J.G., Foekens, J.A., Cardoso, F., Piccart, M.J., Buyse, M., Sotiriou, C., 2007. Strong time dependence of the 76-gene prognostic signature for node-negative breast cancer patients in the TRANSBIG multicenter independent validation series. Clin. Cancer Res. 13, 3207–3214.
di Tomaso, E., London, N., Fuja, D., Logie, J., Tyrrell, J.A., Kamoun, W., Munn, L.L., Jain, R.K., 2009. PDGF-C induces maturation of blood vessels in a model of glioblastoma and attenuates the response to anti-VEGF treatment. PLoS One 4, e5123.
Fagiani, E., Lorentz, P., Kopfstein, L., Christofori, G., 2011. Angiopoietin-1 and -2 exert antagonistic functions in tumor angiogenesis, yet both induce lymphangiogenesis. Cancer Res. 71, 5717–5727.
Folkman, J., 1990. What is the evidence that tumors are angiogenesis dependent? J. Natl. Cancer Inst. 82, 4–6.
Furuhashi, M., Sjoblom, T., Abramsson, A., Ellingsen, J., Micke, P., Li, H., Bergsten-Folestad, E., Eriksson, U., Heuchel, R., Betsholtz, C., Heldin, C.H., Ostman, A., 2004. Platelet-derived growth factor production by B16 melanoma cells leads to increased pericyte abundance in tumors and an associated increase in tumor growth rate. Cancer Res. 64, 2725–2733.
Gibby, K., You, W.K., Kadoya, K., Helgadottir, H., Young, L.J., Ellies, L.G., Chang, Y., Cardiff, R.D., Stallcup, W.B., 2012. Early vascular deficits are correlated with delayed mammary tumorigenesis in the MMTV-PyMT transgenic mouse following genetic ablation of the NG2 proteoglycan. Breast Cancer Res. 14, R67.
Gorantla, B., Asuthkar, S., Rao, J.S., Patel, J., Gondi, C.S., 2011. Suppression of the uPAR-uPA system retards angiogenesis, invasion, and in vivo tumor development in pancreatic cancer cells. Mol. Cancer Res. 9, 377–389.
Guo, P., Hu, B., Gu, W., Xu, L., Wang, D., Huang, H.J., Cavenee, W.K., Cheng, S.Y., 2003. Platelet-derived growth factor-B enhances glioma angiogenesis by stimulating vascular endothelial growth factor expression in tumor endothelia and by promoting pericyte recruitment. Am. J. Pathol. 162, 1083–1093.
Hawighorst, T., Skobe, M., Streit, M., Hong, Y.K., Velasco, P., Brown, L.F., Riccardi, L., Lange-Asschenfeldt, B., Detmar, M., 2002. Activation of the tie2 receptor by angiopoietin-1 enhances tumor vessel maturation and impairs squamous cell carcinoma growth. Am. J. Pathol. 160, 1381–1392.
Hirota, J., Mombaerts, P., 2004. The LIM-homeodomain protein Lhx2 is required for complete development of mouse olfactory sensory neurons. Proc. Natl. Acad. Sci. U.S.A. 101, 8751–8755.
Huang, F.J., You, W.K., Bonaldo, P., Seyfried, T.N., Pasquale, E.B., Stallcup, W.B., 2010. Pericyte deficiencies lead to aberrant tumor vascularizaton in the brain of the NG2 null mouse. Dev. Biol. 344, 1035–1046.
Huber, M.A., Kraut, N., Beug, H., 2005. Molecular requirements for epithelial-mesenchymal transition during tumor progression. Curr. Opin. Cell Biol. 17, 548–558.
Jechlinger, M., Grunert, S., Tamir, I.H., Janda, E., Ludemann, S., Waerner, T., Seither, P., Weith, A., Beug, H., Kraut, N., 2003. Expression profiling of epithelial plasticity in tumor progression. Oncogene 22, 7155–7169.
Jechlinger, M., Sommer, A., Moriggl, R., Seither, P., Kraut, N., Capodiecci, P., Donovan, M., Cordon-Cardo, C., Beug, H., Grunert, S., 2006. Autocrine PDGFR signaling promotes mammary cancer metastasis. J. Clin. Invest. 116, 1561–1570.
Koyama, N., Hart, C.E., Clowes, A.W., 1994. Different functions of the platelet-derived growth factor-alpha and -beta receptors for the migration and proliferation of cultured baboon smooth muscle cells. Circ. Res. 75, 682–691.
Kuzmanov, A., Wielockx, B., Rezaei, M., Kettelhake, A., Breier, G., 2012. Overexpression of factor inhibiting HIF-1 enhances vessel maturation and tumor growth via platelet-derived growth factor-C. Int. J. Cancer 131, E603–E613.
Lehembre, F., Yilmaz, M., Wicki, A., Schomber, T., Strittmatter, K., Ziegler, D., Kren, A., Went, P., Derksen, P.W., Berns, A., Jonkers, J., Christofori, G., 2008. NCAM-induced focal adhesion assembly: a functional switch upon loss of E-cadherin. EMBO J. 27, 2603–2615.
Lin, E.Y., Jones, J.G., Li, P., Zhu, L., Whitney, K.D., Muller, W.J., Pollard, J.W., 2003. Progression to malignancy in the polyoma middle T oncoprotein mouse breast cancer model provides a reliable model for human diseases. Am. J. Pathol. 163, 2113–2126.
Mangale, V.S., Hirokawa, K.E., Satyaki, P.R., Gokulchandran, N., Chikbire, S., Subramanian, L., Shetty, A.S., Martynoga, B., Paul, J., Mai, M.V., Li, Y., Flanagan, L.A., Tole, S., Monuki, E.S., 2008. Lhx2 selector activity specifies cortical identity and suppresses hippocampal organizer fate. Science 319, 304–309.
Marcos-Mondejar, P., Peregrin, S., Li, J.Y., Carlsson, L., Tole, S., Lopez-Bendito, G., 2012. The lhx2 transcription factor controls thalamocortical axonal guidance by specific regulation of robo1 and robo2 receptors. J. Neurosci. 32, 4372–4385.
Mardaryev, A.N., Meier, N., Poterlowicz, K., Sharov, A.A., Sharova, T.Y., Ahmed, M.I., Rapisarda, V., Lewis, C., Fessing, M.Y., Ruenger, T.M., Bhawan, J., Werner, S., Paus, R., Botchkarev, V.A., 2011. Lhx2 differentially regulates Sox9, Tcf4 and Lgr5 in hair follicle stem cells to promote epidermal regeneration after injury. Development 138, 4843–4852.
Mazzone, M., Dettori, D., Leite de Oliveira, R., Loges, S., Schmidt, T., Jonckx, B., Tian, Y.M., Lanahan, A.A., Pollard, P., Ruiz de Almodovar, C., De Smet, F., Vinckier, S., Aragones, J., Debackere, K., Luttun, A., Wyns, S., Jordan, B., Pisacane, A., Gallez, B., Lampugnani, M.G., Dejana, E., Simons, M., Ratcliffe, P., Maxwell, P., Carmeliet, P., 2009. Heterozygous deficiency of PHD2 restores tumor oxygenation and inhibits metastasis via endothelial normalization. Cell 136, 839–851.
Miettinen, P.J., Ebner, R., Lopez, A.R., Derynck, R., 1994. TGF-beta induced transdifferentiation of mammary epithelial cells to mesenchymal cells: involvement of type I receptors. J. Cell Biol. 127, 2021–2036.
Minn, A.J., Gupta, G.P., Siegel, P.M., Bos, P.D., Shu, W., Giri, D.D., Viale, A., Olshen, A.B., Gerald, W.L., Massague, J., 2005. Genes that mediate breast cancer metastasis to lung. Nature 436, 518–524.
Nasarre, P., Thomas, M., Kruse, K., Helfrich, I., Wolter, V., Deppermann, C., Schadendorf, D., Thurston, G., Fiedler, U., Augustin, H.G., 2009. Host-derived angiopoietin-2 affects early stages of tumor development and vessel maturation but is dispensable for later stages of tumor growth. Cancer Res. 69, 1324–1333.

Polyak, K., Weinberg, R.A., 2009. Transitions between epithelial and mesenchymal states: acquisition of malignant and stem cell traits. Nat. Rev. Cancer 9, 265–273.

Porter, F.D., Drago, J., Xu, Y., Cheema, S.S., Wassif, C., Huang, S.P., Lee, E., Grinberg, A., Massalas, J.S., Bodine, D., Alt, F., Westphal, H., 1997. Lhx2, a LIM homeobox gene, is required for eye, forebrain, and definitive erythrocyte development. Development 124, 2935–2944.

Rhee, H., Polak, L., Fuchs, E., 2006. Lhx2 maintains stem cell character in hair follicles. Science 312, 1946–1949.

Roberson, M.S., Schoderbek, W.E., Tremml, G., Maurer, R.A., 1994. Activation of the glycoprotein hormone alpha-subunit promoter by a LIM-homeodomain transcription factor. Mol. Cell Biol. 14, 2985–2993.

Roy, A., de Melo, J., Chaturvedi, D., Thein, T., Cabrera-Socorro, A., Houart, C., Meyer, G., Blackshaw, S., Tole, S., 2013. LHX2 is necessary for the maintenance of optic identity and for the progression of optic morphogenesis. J. Neurosci 33, 6877–6884.

Sugimoto, H., Mundel, T.M., Kieran, M.W., Kalluri, R., 2006. Identification of fibroblast heterogeneity in the tumor microenvironment. Cancer Biol. Ther. 5, 1640–1646.

ten Freyhaus, H., Huntgeburth, M., Wingler, K., Schnitker, J., Baumer, A.T., Vantler, M., Bekhite, M.M., Wartenberg, M., Sauer, H., Rosenkranz, S., 2006. Novel Nox inhibitor VAS2870 attenuates PDGF-dependent smooth muscle cell chemotaxis, but not proliferation. Cardiovasc. Res. 71, 331–341.

Thiery, J.P., Acloque, H., Huang, R.Y., Nieto, M.A., 2009. Epithelial–mesenchymal transitions in development and disease. Cell 139, 871–890.

Thiery, J.P., Sleeman, J.P., 2006. Complex networks orchestrate epithelial–mesenchymal transitions. Nat. Rev. Mol. Cell Biol. 7, 131–142.

Thommen, R., Humar, R., Misevic, G., Pepper, M.S., Hahn, A.W., John, M., Battegay, E.J., 1997. PDGF-BB increases endothelial migration on cord movements during angiogenesis in vitro. J. Cell Biochem. 64, 403–413.

Tiwari, N., Meyer-Schaller, N., Arnold, P., Antoniadis, H., Pachkov, M., van Nimwegen, E., Christofori, G., 2013a. Klf4 is a transcriptional regulator of genes critical for EMT, including Jnk1 (Mapk8). PLoS One 8, e57329.

Tiwari, N., Tiwari, V.K., Waldmeier, L., Balwierz, P.J., Arnold, P., Pachkov, M., Meyer-Schaller, N., Schubeler, D., van Nimwegen, E., Christofori, G., 2013b. Sox4 is a master regulator of epithelial–mesenchymal transition by controlling ezh2 expression and epigenetic reprogramming. Cancer Cell 23, 768–783.

Tornqvist, G., Sandberg, A., Hagglund, A.C., Carlsson, L., 2010. Cyclic expression of lhx2 regulates hair formation. PLoS Genet 6, e1000904.

Trimboli, A.J., Fukino, K., de Bruin, A., Wei, G., Shen, L., Tanner, S.M., Creasap, N., Rosol, T.J., Robinson, M.L., Eng, C., Ostrowski, M.C., Leone, G., 2008. Direct evidence for epithelial–mesenchymal transitions in breast cancer. Cancer Res. 68, 937–945.

Usami, Y., Satake, S., Nakayama, F., Matsumoto, M., Ohnuma, K., Komori, T., Semba, S., Ito, A., Yokozaki, H., 2008. Snail-associated epithelial–mesenchymal transition promotes oesophageal squamous cell carcinoma motility and progression. J. Pathol. 215, 330–339.

Vergara, D., Merlot, B., Lucot, J.P., Collinet, P., Vinatier, D., Fournier, I., Salzet, M., 2010. Epithelial–mesenchymal transition in ovarian cancer. Cancer Lett. 291, 59–66.

Waldmeier, L., Meyer-Schaller, N., Diepenbruck, M., Christofori, G., 2012. Py2T murine breast cancer cells, a versatile model of TGFbeta-induced EMT in vitro and in vivo. PLoS One 7, e48651.

Wandzioch, E., Kolterud, A., Jacobsson, M., Friedman, S.L., Carlsson, L., 2004. Lhx2−/− mice develop liver fibrosis. Proc. Natl. Acad. Sci. U.S.A. 101, 16549–16554.

Weber, M., Hellmann, I., Stadler, M.B., Ramos, L., Paabo, S., Rebhan, M., Schubeler, D., 2007. Distribution, silencing potential and evolutionary impact of promoter DNA methylation in the human genome. Nat. Genet. 39, 457–466.

Weidner, N., Semple, J.P., Welch, W.R., Folkman, J., 1991. Tumor angiogenesis and metastasis–correlation in invasive breast carcinoma. N. Engl. J. Med. 324, 1–8.

Xu, Y., Baldassare, M., Fisher, P., Rathbun, G., Oltz, E.M., Yancopoulos, G.D., Jessell, T.M., Alt, F.W., 1993. LH-2: a LIM/homeodomain gene expressed in developing lymphocytes and neural cells. Proc. Natl. Acad. Sci. U.S.A. 90, 227–231.

Yilmaz, M., Maass, D., Tiwari, N., Waldmeier, L., Schmidt, P., Lehembre, F., Christofori, G., 2011. Transcription factor Dlx2 protects from TGFbeta-induced cell-cycle arrest and apoptosis. EMBO J. 30, 4489–4499.

Yu, J., Moon, A., Kim, H.R., 2001. Both platelet-derived growth factor receptor (PDGFR)-alpha and PDGFR-beta promote murine fibroblast cell migration. Biochem. Biophys. Res. Commun. 282, 697–700.

Zhao, Y., Mailloux, C.M., Hermesz, E., Palkovits, M., Westphal, H., 2010. A role of the LIM-homeobox gene Lhx2 in the regulation of pituitary development. Dev. Biol. 337, 313–323.